

# Design, Fabrication and Characterization of a Novel Piezoresistive Pressure Sensor for Blast Waves Monitoring

K. Sanchez, B. Achour, J. Riondet, L. Anglade,  
M. Carrera, A. Coustou, A. Lecestre, S. Charlot,  
H. Aubert, P. Pons

CNRS-LAAS, Toulouse University  
Toulouse, France  
ksanchezba@laas.fr, bachour@laas.fr, jriondet@laas.fr,  
laurene.anglade@outlook.fr,  
miguel.carrera.iz@hotmail.com, acoustou@laas.fr,  
alecestre@laas.fr, scharlot@laas.fr, haubert@laas.fr,  
ppons@laas.fr

M. Lavayssière, A. Lefrançois, J. Luc

CEA-DAM  
Gramat, France  
maylis.lavayssiere@cea.fr, alexandre.lefrancois@cea.fr,  
jerome.luc@cea.fr,

**Abstract**— In several side-on configurations, the monitoring of blast wave requires sensor with very low response time ( $< 1 \mu\text{s}$ ). The sensing area of commercial sensors are too high to fulfill this specification. New transducers are focused on miniature membrane (diameter  $< 100 \mu\text{m}$ ), but with optical transduction which suffers from low integration capabilities for multiple transducers. In this communication, a miniature piezoresistive pressure transducer based on silicon membrane and silicon gauges is designed and fabricated. Shock tube characterizations of the sensor have shown promising dynamic behavior, with a rise time of 30 ns and a response time lower than  $1 \mu\text{s}$  thanks to the membrane fundamental resonant frequency of 20 MHz. Undesirable mechanical effects leading to the response drift after  $1 \mu\text{s}$  are discussed and interpreted as the result of the holder deformation.

**Keywords** – shockwave ; air blast ; pressure sensor

## I. INTRODUCTION

Blast waves monitoring is required for many civilian and military applications, and especially for explosives characterization. In this case, and for supersonic shock wave, the side-on over-pressure (i.e., when the transducer surface is parallel to the flow velocity) reaches quasi-instantaneously ( $< 10 \text{ ns}$ ) a maximum  $P_{\text{max}}$  (from several bar to several ten of bar) and then decreases rapidly (from several ten of microseconds to several hundred of microseconds).

In order to analyze the effect of supersonic shock wave on systems, the accurate estimation of  $P_{\text{max}}$  is mandatory [1]. For several setup configurations (mass of explosive, distance between source and sensor), the over-pressure decrease phase is lower than  $100 \mu\text{s}$ . In these cases, sensors with response time lower than  $1 \mu\text{s}$  are required.

The pressure sensors commercially available and suitable for pyrotechnic applications, use mainly piezoelectric transducers with ceramic thick disk [2][3] or polymer thin film [4]. The typical response time of such sensors is about several microseconds for side-on configuration. High response times is mainly due to the large diameter ( $> 900 \mu\text{m}$ ), of used piezoelectric layers, in order to produce enough electrical charges.

In order to reduce the response time, micro-membranes with a diameter lower than  $100 \mu\text{m}$  and based on optical transduction have been reported in [5]-[8]. These sensors have good dynamic performances with frequency bandwidth often higher than 10 MHz. But the optical transduction requires complex technological steps and does not facilitate the high integration of multiple sensors.

Recently, we proposed a transducer using a miniature monocrystalline silicon membrane and silicon piezoresistive gauges [9]-[10]. The objective was to combine the advantage of miniature membrane (sensing diameter  $< 100 \mu\text{m}$ ) and the high integration of electronic transduction. In this paper, we report the design, fabrication and characterization of this transducer, and we explore the unexpected and undesirable mechanical response observed beyond  $1 \mu\text{s}$ .

The paper is organized as follows. The design of the transducer is presented in Section 2. The Section 3 is dedicated to the fabrication of the transducer. The simulated (COMSOL) static pressure response of the transducer is given in Section 4. Finally, Section 5 describes the dynamic pressure response of the sensor using a shock tube.

## II. TRANSDUCER DESIGN

The topology of the transducer is displayed in Figure 1 and Figure 2.

A N-type monocrystalline  $5 \mu\text{m}$  thick silicon membrane is used for the mechanical transducer. This membrane is obtained by releasing the top layer of a Silicon-On-Insulator (SOI) substrate. Its shape is rectangular with targeted width  $W_M = 30 \mu\text{m}$  and length  $L_M = 90 \mu\text{m}$ .

The electrical transducer is provided by P-type monocrystalline silicon gauges, which are inserted at the center of the N-type silicon membrane and are distributed using the Wheatstone bridge configuration. The inter-isolation of the gauges is obtained from the reverse polarization of the P/N junction. The targeted gauges width is  $W_J = 1 \mu\text{m}$  and length  $L_J = 5 \mu\text{m}$ .

The pressure is applied on the top side of the membrane and a reference cavity with vacuum is located at the bottom side of the membrane.

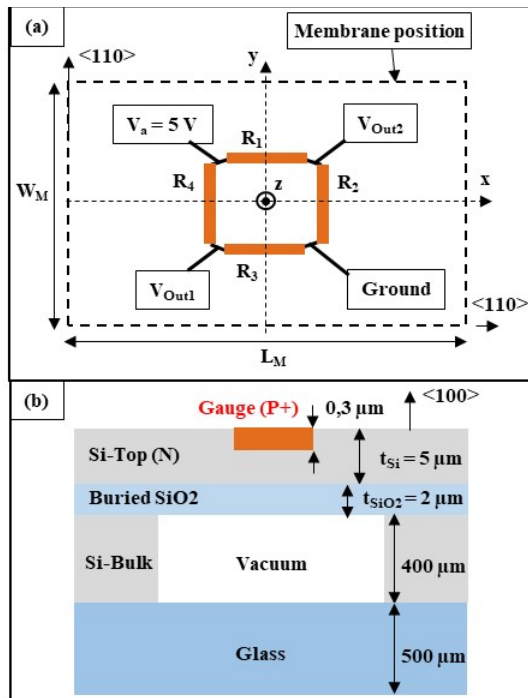


Figure 1. (a) Top view of the Wheatstone bridge reported on the membrane surface, (b) Cross sectional diagram of the transducer.

### III. TRANSDUCER FABRICATION

This section describes, first of all, the different technological steps required for the fabrication of the transducer. Electrical characterization of the gauges is then discussed. The last part is dedicated to the measurement of the membrane dimensions.

#### A. Technological fabrication steps

The transducer fabrication uses SOI wafers, whose characteristics are given in Table 1. The transducer on its metallic holder is shown in Figure 3.

TABLE 1. SOI WAFERS CHARACTERISTICS PROVIDED BY THE SUPPLIER

Si-top	Orientation	(100)
	Type	N
	Doping level	$4.8 \cdot 10^{15}$ to $1.6 \cdot 10^{15}$ at/cm <sup>3</sup>
	Thickness	$(5.0 \pm 0.5)$ μm
Buried SiO <sub>2</sub>	Thickness	$(2.0 \pm 0.1)$ μm
Si Bulk	Orientation	(100)
	Thickness	$(400 \pm 15)$ μm

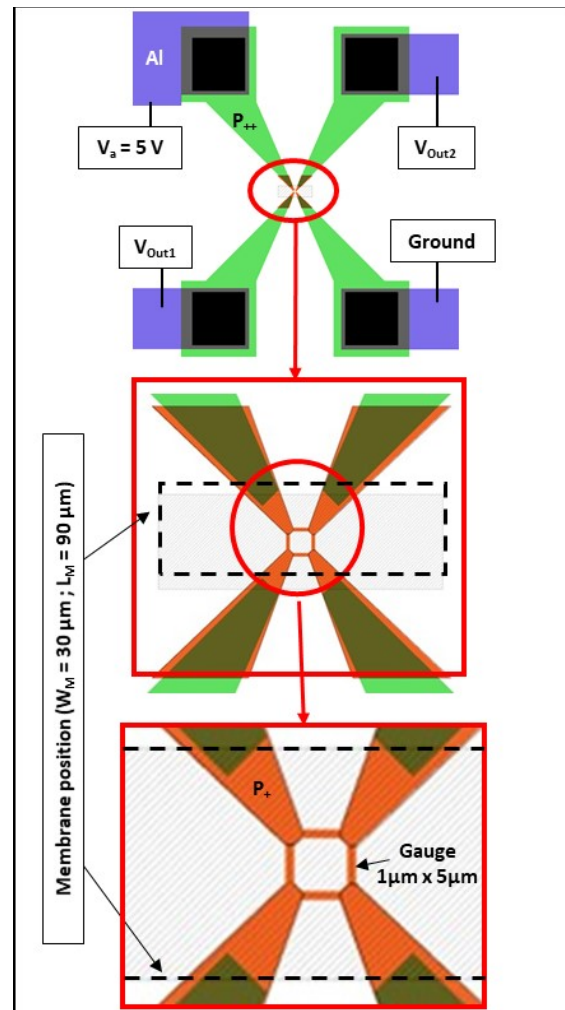


Figure 2. Top view of the mask used for the technological process

The technological process starts with the growing of a 40 nm thick thermal silicon dioxide (SiO<sub>2</sub>) layer. Boron and phosphorus implantations are then performed respectively for the low resistivity interconnections between gauges and metallic lines and for the electrical contact on SiN-top. Both implantations are done with the same parameters (Energy = 50 keV, Dose = 10<sup>16</sup> at/cm<sup>2</sup>). The activation annealing of dopants is then performed during one hour at 1000 °C.

The next step is dedicated to the gauge's fabrication with boron implantation (Energy = 20 keV, Dose = 5\*10<sup>14</sup> at/cm<sup>2</sup>). The activation annealing of dopants is performed with rapid thermal annealing during one minute at 1000 °C, in order to hold the dopant close to the membrane surface where the stress is maximal and then to maximize the transducer sensitivity. The surface concentration is of 3.5 10<sup>19</sup> at/cm<sup>3</sup>, which consists of a good trade-off between gauge sensitivities to strain and temperature. The junction depth is of 0.3 μm.

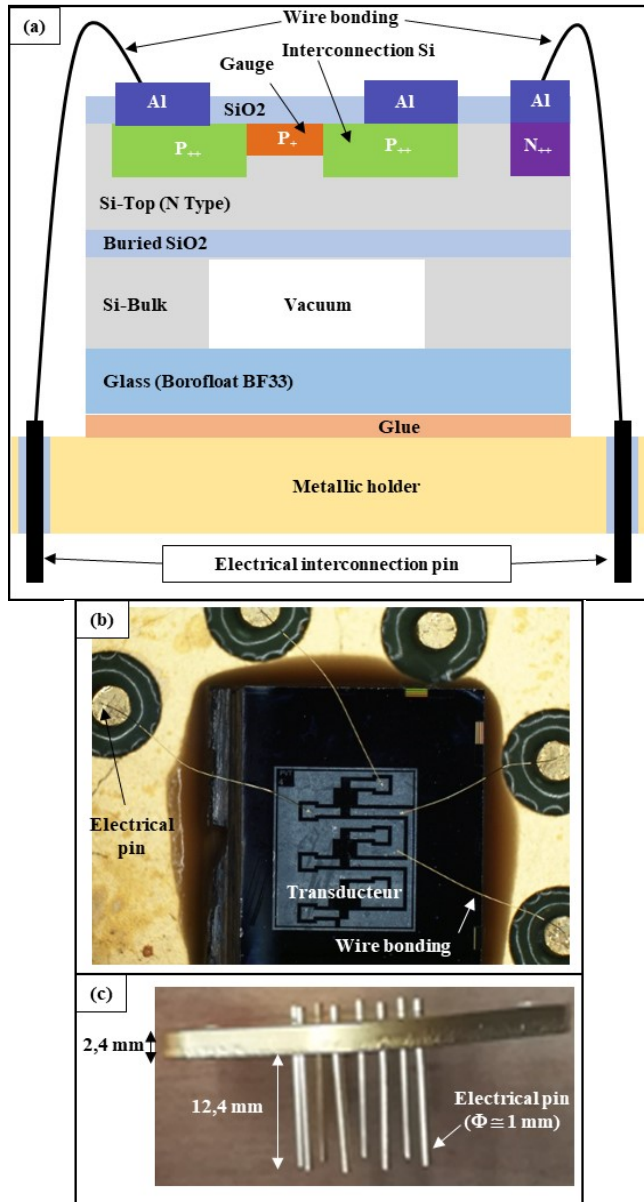


Figure 3. (a) Cross section diagram of the transducer on its metallic holder, (b) Top view of the transducer glued to the metallic holder, (c) View of TO3 metallic holder.

Next, the deposition of a 350 nm thick SiO<sub>2</sub> layer is performed at 300°C by Plasma Enhanced Chemical Vapor Deposition to provide enough electrical isolation between gauges and future metallic interconnections. After contact opening by liquid etching of the SiO<sub>2</sub> layer, a 500 nm thick aluminum layer is deposited by thermal evaporation for metallic interconnections. The silicon membrane is then released by using a Deep Reactive Ionic Etching (DRIE) of Si-bulk from back-side, up to the buried-SiO<sub>2</sub> etch-stop layer.

After the anodic bonding of the glass substrate on the silicon back side, the wafer is cut and the die is glued on a metallic holder. Wire bonding is finally performed between transducer pads and holder pin.

### B. Electrical characteristics of the fabricated gauges

The transducer resistance  $R_{\text{Transd}}$  (between  $V_{\text{out1}}$  and  $V_{\text{out2}}$ ), measured before the wafer dicing, is of  $(2990 \pm 100) \Omega$ . This measurement result is slightly lower than the simulated one ( $3650 \Omega$ ) obtained from COMSOL software, using mask dimension opening of  $W_J = 1 \mu\text{m}$  and  $L_J = 5 \mu\text{m}$ . With these dimensions, the gauge resistance  $R_J$  is of  $1380 \Omega$ . The difference with the transducer resistance  $R_{\text{Transd}}$  is due to the access resistance (mainly the P<sub>+</sub> interconnection between the gauges and the P<sub>++</sub> interconnection).

As shown on Figure 4, the final dimensions of the fabricated gauge are impacted by the photoresist lateral under-etching  $d_{\text{sur}} = (110 \pm 40) \text{ nm}$  (Figure 4-a) and also by the boron diffusion  $d_{\text{lat}}$  (about 130 nm) during annealing, corresponding to a boron doping level of  $1 \cdot 10^{19} \text{ at/cm}^3$  (Figure 4-b). The final gauge width  $W_{Jf}$  and length  $L_{Jf}$  are respectively of  $1.5 \mu\text{m}$  and  $4.5 \mu\text{m}$  (equations (1) and (2)).

$$W_{Jf} = W_J + 2 \cdot d_{\text{sur}} + 2 \cdot d_{\text{lat}} \quad (1)$$

$$L_{Jf} = L_J - 2 \cdot d_{\text{sur}} - 2 \cdot d_{\text{lat}} \quad (2)$$

Using the dimensions  $W_{Jf}$  and  $L_{Jf}$  (instead of the dimension of the mask opening  $W_J$  and  $L_J$ ), a very good agreement is obtained between the simulated transducer resistance  $R_{\text{Transd}}$  ( $3110 \Omega$ ) and the measured resistance ( $2990 \Omega \pm 100 \Omega$ ).

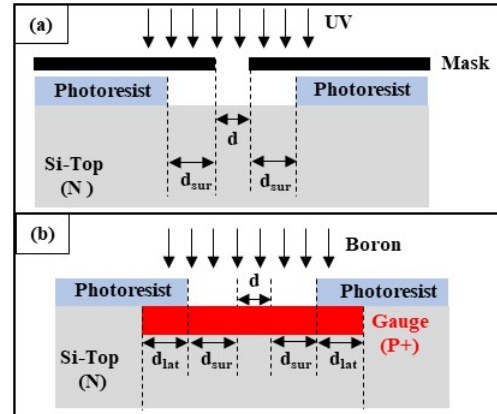


Figure 4. Cross section diagram of gauge showing lateral dimension increase due to the (a) Photoresist etching and (b) Boron diffusion.

### C. Membrane dimensions

As shown in Figure 5, the membrane width is higher than the mask opening. This originates in the lateral under-etching of the 40 μm thick photoresist, the non-ideal vertical DRIE etching of silicon and finally the lateral under-etching of silicon related to the accumulation of chemical species, when the buried SiO<sub>2</sub> layer is reached.

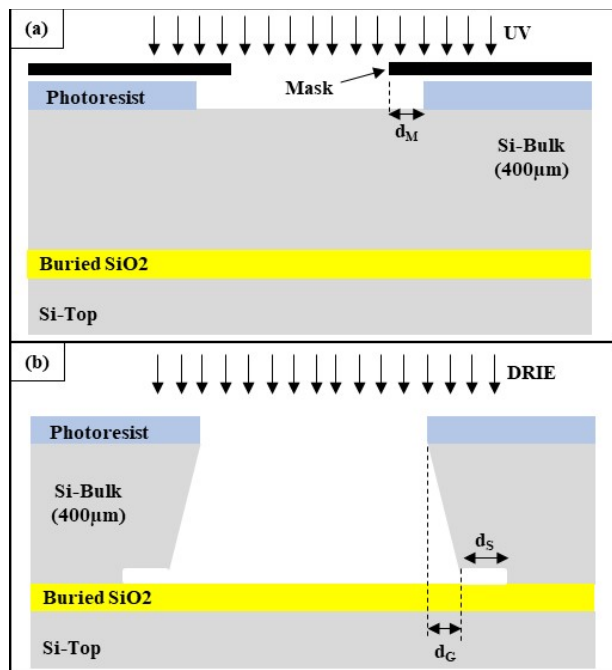


Figure 5. Cross section diagram of membrane showing lateral dimension increase due to the (a) Photoresist etching and (b) Si DRIE etching.

The dimensions of the fabricated membranes are measured on several samples using Focus Ion Beam (FIB) etching, for cross section realization, and Scanning Electron Microscopy (SEM), for dimensional measurements (Figure 6). The results obtained are given in Table 2.

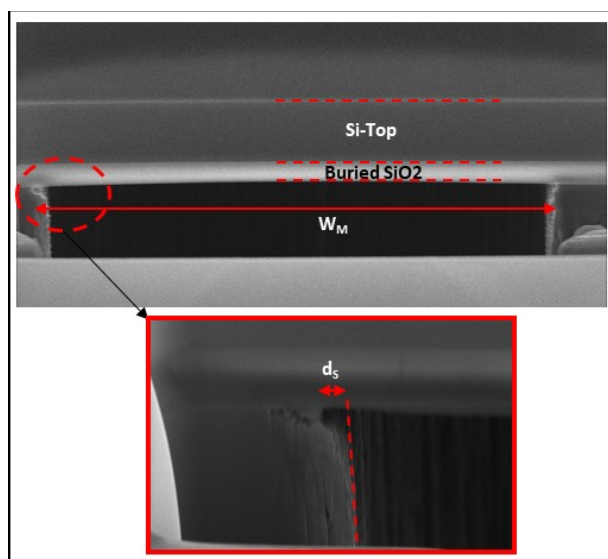


Figure 6. Cross section MEB photography after DRIE etching.

TABLE 2. MEMBRANE DIMENSIONS MEASUMED by SEM

Si-top thickness ( $\mu\text{m}$ )	$5.0 \pm 0.2$ to $5.7 \pm 0.2$
Buried SiO <sub>2</sub> thickness ( $\mu\text{m}$ )	$1.8 \pm 0.2$ to $2.0 \pm 0.2$
Membrane width ( $\mu\text{m}$ )	$39.5 \pm 0.2$ to $42.5 \pm 0.2$

The Si-top and buried SiO<sub>2</sub> measured layers thicknesses are in good agreement with the characteristics provided by the supplier (Table 1). The average membrane width is of 41  $\mu\text{m}$ , that is, 37 % larger than the mask width, with a scattering of  $\pm 3.6$  %.

#### IV. SIMULATED RESPONSE OF THE TRANSDUCER TO STATIC PRESSURE

COMSOL simulations were performed to predict the static transducer performances. The full design was considered (Figure 1 and Figure 2) with two membrane dimensions corresponding to the lowest and the highest mechanical stiffness given by the measured membrane dimensions (see Table 2). The static pressure sensitivity and the fundamental mechanical resonant frequency are reported in Table 3.

TABLE 3. SIMULATED (COMSOL) PERFORMANCES OF THE TRANSDUCER

Case-1:  $t_{\text{Si}} = 4.8 \mu\text{m}$ ,  $t_{\text{SiO}_2} = 2 \mu\text{m}$ ,  $W_M = 43 \mu\text{m}$ ,  $L_M = 103 \mu\text{m}$   
 Case-2:  $t_{\text{Si}} = 5.9 \mu\text{m}$ ,  $t_{\text{SiO}_2} = 2 \mu\text{m}$ ,  $W_M = 39 \mu\text{m}$ ,  $L_M = 99 \mu\text{m}$

	Case 1	Case 2
Static pressure sensitivity $S_{\text{Transd}}$ ( $\mu\text{V/V/bar}$ )	209	138
Fundamental mechanical resonant frequency $F_0$ (MHz)	25.7	34.3

The simulated static pressure sensitivity is between 138  $\mu\text{V/V/bar}$  and 209  $\mu\text{V/V/bar}$ . The uncertainty on the transducer sensitivity is then of  $\pm 20.5$  %. The simulated fundamental mechanical resonant frequency of the membrane ranges from 25.7 MHz to 34.3 MHz, corresponding to an uncertainty of  $\pm 14.3$  %.

#### V. SHOCK TUBE CHARACTERIZATION OF THE FABRICATED SENSOR

This section describes, first of all, the setup used for the dynamic pressure characterization of the fabricated sensor. Then the sensor response, to a pressure step, is given. The last part analyses the sensor drift; that appears after 1  $\mu\text{s}$ .

##### A. Setup description

The setup used for the dynamic pressure characterization of the sensor is illustrated on Figure 7.

A 2.7 m length and 11 cm inner-diameter metrological shock tube allows generating a pressure step with a rise time lower than 10 ns. The driver section is filled with nitrogen gas, while the driven section is at atmospheric pressure. The diaphragm, which separates the two sections, is a standard nickel rupture disc that opens fully and responds within milliseconds to the applied overpressure. Its rupture creates a shock wave that propagates along the tube until reflections by the metallic end-wall of the tube, where the pressure is measured both by our transducer and by using a commercial reference sensor (PCB Piezotronics 134A24) for comparison purpose.

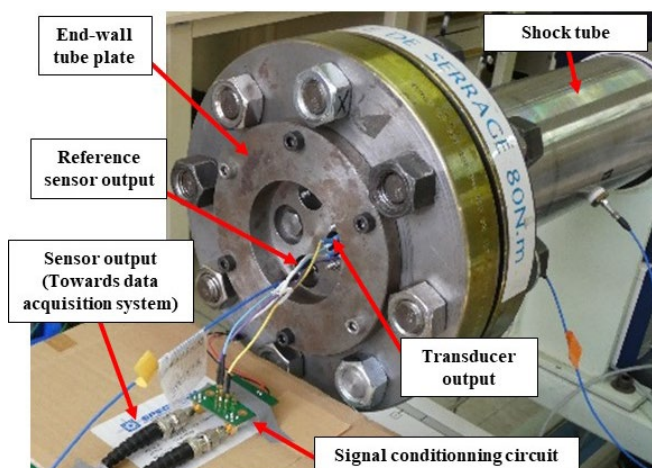


Figure 7. Experimental setup for dynamic pressure characterization

The transducer output is connected to a conditioning circuit through a length (10 cm) of shielded wires. The static gain of this circuit is of 0.9, with a cut-of frequency of 35 MHz. The sampling frequency of the data acquisition system is of 100 MHz.

*B. Measured sensor response to a pressure step*

The measured sensor response (at the output of the conditioning circuit) to a 10 bar pressure step is shown in Figure 8.

A typical damped oscillation is obtained in the first micro-second due to the excitation of the fundamental mechanical resonant mode of the membrane. From this measurement result, we can derive the main transducer characteristics: the rise time of 30 ns, the response time lower than 1  $\mu$ s and the steady-state pressure sensitivity around 200  $\mu$ V/V/bar (assuming a gain of 0.9 from the conditioning circuit). This sensitivity is then in good agreement with the simulated value.

The fundamental resonant frequency of 20.4 MHz is also in good agreement with the simulated value, as shown in Figure 9, which displays the spectral analysis of the measured sensor response. But beyond 1  $\mu$ s, we observe that an unexpected drift appears. The next section is devoted to the interpretation of this drift.

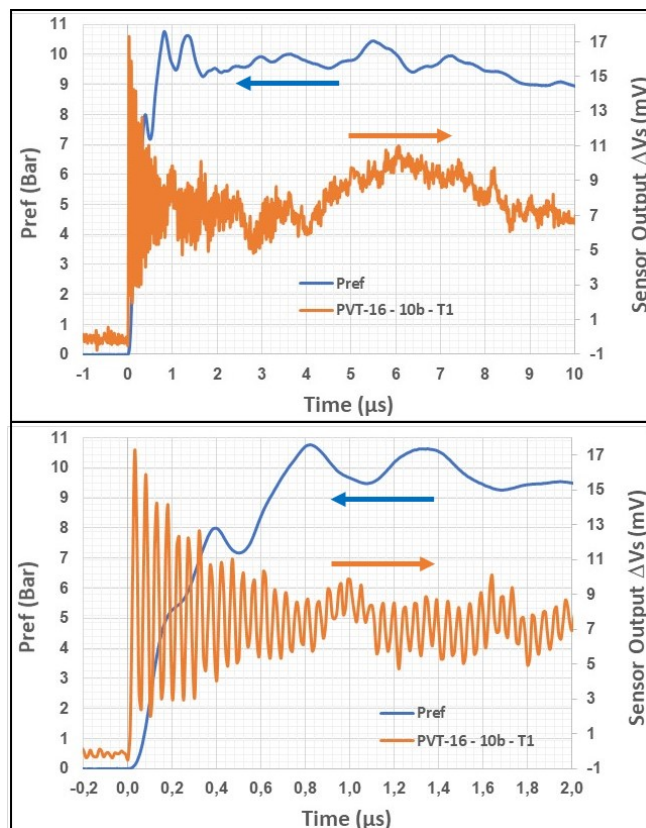


Figure 8. Measured sensor response to a 10 bar step pressure (orange line) and reference sensor (blue line)

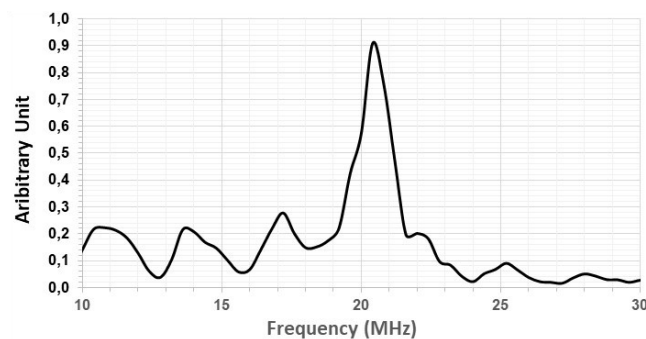


Figure 9. Spectral analysis of the sensor response derived from measurement

*C. Analysis of the observed sensor drift*

The sensor response to a 10 bar pressure step is shown in Figure 10 using four different measurement configurations.

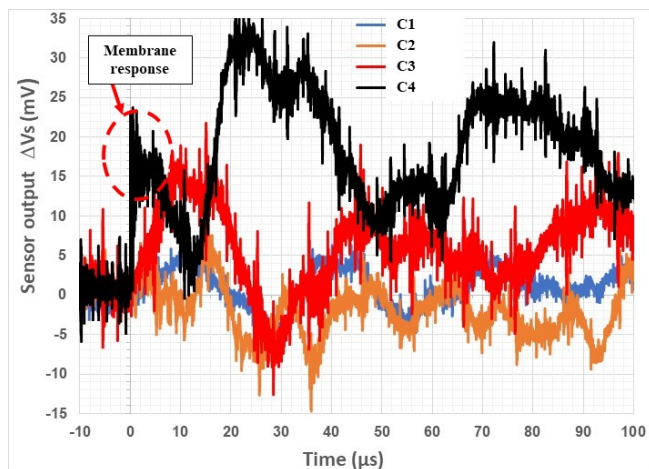


Figure 10. Sensor output with a 10 bar pressure step.  
 Configuration C1: Without membrane - With Cover  
 Configuration C2: Without membrane - Without Cover  
 Configuration C3: With membrane - With Cover  
 Configuration C4: With membrane - Without Cover

In configuration C1, the Si-Bulk is not removed below the gauges and a metallic cover is used to avoid direct shock wave effect (blue color). In this configuration, only indirect strain is applied on the gauges, without the membrane amplification. A slow variation of the sensor response is observed, with an amplitude of  $\pm 5$  mV.

The same transducer is used in the configuration C2, but without the metallic cover (orange color). Compared with configuration C1, the sensor response is not significantly modified, but a higher amplitude ( $\pm 10$  mV) is observed due to the direct impact of the shock wave under the gauge and/or the mechanical stiffening of the metallic holder by the metallic cover.

In the configuration C3, the response of a transducer with a membrane and a metallic cover is measured (red color). The large undesirable effect observed in the response (around 3 times of one recorded in the configuration C1) can be explained by the mechanical deformations of the metallic holder, which are transmitted to the membrane and then amplified.

Finally, the same transducer used in the configuration C3 is measured in configuration C4, but without the metallic cover (black color). As expected, the membrane response is apparent in the first micro-seconds, and consequently, the drift occurs.

## VI. CONCLUSIONS AND FUTURE WORKS

The characterization of supersonic shock wave produced by explosives requires sensor with response time lower than  $1 \mu\text{s}$  in order to quantify accurately the maximum overpressure in several side-on configurations. With sensing diameter greater than  $900 \mu\text{m}$ , the commercial sensors are not able to fulfill this specification. Researches are focused on miniature membranes (diameter  $< 100 \mu\text{m}$ ), but they very often applied an optical transduction, which requires complex

technological steps and are not compatible with the integration of several transducers on the same chip.

We proposed here a pressure transducer using a miniature silicon membrane and piezoresistive gauges in order to combine the advantage of miniature sensing area and microelectronic integration. A miniature piezoresistive pressure sensor was designed, fabricated and characterized within a shock tube. The proposed sensor has a very low rise time (about 30 ns) and a short response time (about  $1 \mu\text{s}$ ), thanks to the high fundamental mechanical resonant mode of the membrane (close to 20 MHz). Mechanical parasitic effects, that leads to large drift after few microseconds, were explored and identified. This effect was interpreted as the result of the metallic holder deformation due to the shock wave. New packaging with higher mechanical stiffness will be designed in order to reduce these undesirable effects in the pressure response of the transducer.

## ACKNOWLEDGMENT

This work was partially funded by Occitanie Region, France, through the COCNANO project and was supported by LAAS-CNRS micro and nanotechnologies platform members of the French RENATECH network.

## REFERENCES

- [1] L. Walter, "Air-blast and the Science of Dynamic Pressure Measurements", *Sound and Vibration*, Vol. 38, No 12, pp 10-17, Dec. 2004.
- [2] Piezotronics PCB [<https://www.pcb.com/sensors-for-test-measurement/pressure-transducers/blast-transducers>].
- [3] Kistler [<https://www.kistler.com/?type=669&fid=85810&model=document>].
- [4] Muller Instrument [<https://mueller-instruments.de/en/pressure-measurement/pressure-sensor-m/>].
- [5] N. Wu et al. "An ultra-fast fiber optic pressure sensor for blast event measurements", *Measurements Sciences and Technologies*, Vol. 23, No 5, April 2012, doi:10.1088/0957-0233/23/5/055102.
- [6] X. Zou, N. Wu, Y. Tian, C. Niezrecki, J. Chen, X. Wang, "Rapid miniature fiber optic pressure sensors for blast wave measurements", *Optics and lasers in Engineering*, Vol. 51, No 2, pp 134-139, Feb. 2013, doi: 10.1016/j.optlaseng.2012.09.001.
- [7] Z. Wang, G. Wen, Z. Wu, J. Yang, L. Chen, W. Liu, "Fiber optic method for obtaining the peak reflected pressure of shock wave", *Optic Express*, Vol. 28, No 12, June 2018, doi: 10.1364/OE.26.015199.
- [8] C. Chu, J. Wang, J. Qiu, "Miniature High-Frequency Response, High-Pressure-Range Dynamic Pressure Sensor Based on All-Silica Optical Fiber Fabry-Perot Cavity", *IEEE Sensor Journal*, Vol. 21, No 12, pp 13296-13304, June 2021, doi: 10.1109/JSEN.2021.3068456.
- [9] J. Riondet et al. "Design of air blast pressure sensors based on miniature silicon membrane and piezoresistive gauges", *Journal of Physics: Conference Series*, Vol. 922, Aug. 2017, doi: 10.1088/1742-6596/922/1/012019.
- [10] J. Veyrunes et al., "Transient response of miniaturized piezoresistive sensors for side-on pressure shockwave", *Proc. Design, Test, Integration & Packaging of MEMS/MOEMS*, 12-15 May 2019, Paris, France, doi: 10.1109/DTIP.2019.8752911.